Available online at www.sciencedirect.com
ScienceDirect
Ceramics International 35 (2009) 1103–1108
CERAMICS INTERNATIONAL
www.elsevier.com/locate/ceramint

Sonochemical preparation of $PbWO_4$ crystals with different morphologies

Titipun Thongtem [a,*], Sulawan Kaowphong [b], Somchai Thongtem [b]

[a] Department of Chemistry, Faculty of Science, Chiang Mai University, Hauy-Kaew Road, Chiang Mai 50200, Thailand
[b] Department of Physics, Faculty of Science, Chiang Mai University, Chiang Mai 50200, Thailand

Received 17 July 2007; received in revised form 15 February 2008; accepted 10 May 2008
Available online 19 July 2008

Abstract

$PbWO_4$ was prepared from $Na_2WO_4{\cdot}2H_2O$ and $Pb(OAc)_2{\cdot}3H_2O$ in a solution containing a cationic surfactant (*N*-cetyl pyridinium chloride) using the sonochemical process (ultrasonic irradiation). The product morphologies, characterized using scanning electron microscopy (SEM) and transmission electron microscopy (TEM), were controlled by the surfactant, pH values and ultrasonic irradiation times. X-ray diffraction (XRD) and selected area electron diffraction (SAED) studies revealed diffraction patterns in good agreement with the simulation model, along with Fourier transform infrared (FTIR) and Raman analyses showed a W–O stretching band consistent with tetragonal $PbWO_4$. Photoluminescent properties of the pine tree shaped products were also investigated.

Keywords: Lead tungstate; Sonochemical process; *N*-Cetyl pyridinium chloride; Pine tree shape

1. Introduction

$PbWO_4$ is one of the most interesting tungstates and it has found wide use in applications such as electromagnetic calorimetry, excitonic luminescence, thermoluminescence and stimulated Raman scattering behavior [1–3]. A variety of preparation processes have been used to produce different shapes and sizes which strongly affect the material's properties. These processes include synthesis with and without using organic additives, such as microemulsion-based synthesis [4,5], wet chemistry methods [3,6,7], microwave-assisted synthesis [8,9], sonochemical processes [2] and hydrothermal reactions [10]. Surfactants have been added in some of these processes and it is believed that they function as shape directors in product formations [6]. Other parameters, such as pH, temperature, prolonged reaction time and solvent system, can play a role in the formation of different shapes and sizes as well.

Several groups have reported the preparation of $PbWO_4$ using the sonochemical process that yields a variety of shapes: polyhedra, spindle-like and dot-shaped nanostructures [2], hollow spindle [11], and Sb(III)-doped single crystals [12]. The purpose of the present research was to sonochemically prepare $PbWO_4$ in a solution containing *N*-cetyl pyridinium chloride (a cationic surfactant) and classify and examine the resulting structures. The effects of pH and irradiation times on the morphologies have been investigated. An unusual pine tree shaped product, not previously reported from sonochemical studies, is a promising material that contains a number of defects having influence on the luminescent intensity [5].

2. Experiment

All chemicals were of reagent grade. Three solutions were prepared by separately dissolving 0.003 mol $Na_2WO_4{\cdot}2H_2O$, 0.005 mol *N*-cetyl pyridinium chloride (a cationic surfactant) and 0.003 mol $Pb(OAc)_2{\cdot}3H_2O$ in 20 ml de-ionized water each. The $Na_2WO_4{\cdot}2H_2O$ and *N*-cetyl pyridinium chloride solutions were mixed for 30 min under ultrasonic irradiation (sonochemical process). Then the $Pb(OAc)_2{\cdot}3H_2O$ solution was added and the pH was adjusted to be in the range of 3–11. Ultrasonic irradiation was carried out for 1–5 h, resulting in the gradual formation of white precipitates with different shapes and sizes. The crystals were washed with water and ethanol, and

* Corresponding author. Tel.: +66 53 941922x611; fax: +66 53 892277.
E-mail addresses: ttpthongtem@yahoo.com, ttpthongtem@hotmail.com (T. Thongtem).

0272-8842/$34.00
doi:10.1016/j.ceramint.2008.05.007

dried at 80 °C for 24 h for further analysis. The final products were analyzed using X-ray diffraction (XRD) operating at 20 kV, 15 mA, using the Kα line from a Cu target, transmission electron microscopy (TEM) as well as selected area electron diffraction (SAED) operated at 200 kV, scanning electron microscopy (SEM) operated at 15 kV, Fourier transform infrared (FTIR) with KBr as a diluting agent and operated in the range 400–4000 cm^{-1}, a Raman spectrometer using 50 mW Ar Laser with $\lambda = 514.5$ nm, and a luminescence spectrometer using a 300 nm exciting wavelength. In addition, diffraction patterns were simulated using CaRIne Crystallography 3.1 software [13] and compared with those interpreted from the experimental results.

3. Results and discussion

XRD spectra of all the products (Fig. 1) correspond to $PbWO_4$ with tetragonal stolzite structure [1,14]. Its space group is $I4_1/a$. The unit cell parameters are $a = b = 0.5445$ nm, $c = 1.2050$ nm, and $\alpha = \beta = \gamma = 90°$. The spectra diffracted from crystallographic planes of the products are (1 1 2), (0 0 4), (2 0 0), (1 2 1), (2 0 4), (2 2 0), (1 1 6), (3 1 2) and (2 2 4). The strongest intensity diffracted from (1 1 2) plane and is at $2\theta = 27.5°$. The spectra are very sharp showing that the product was composed of a number of crystals. No other characteristic peaks of impurities were detected showing that each product is a pure phase. By mixing $Na_2WO_4{\cdot}2H_2O$ and surfactant (positively charge), $(WO_4)^{2-}$ anions were possibly coordinated the surfactant molecules to form surfactant–tungstate complexes. The addition of $Pb(OAc)_2{\cdot}3H_2O$ into the solution containing the surfactant–tungstate complexes under the assistance of ultrasonic irradiation led to the substitution of the surfactant by Pb^{2+} cations. Once $PbWO_4$ nuclei (very fine particles) formed, they came together to form crystalline solids. The surfactant may have been selectively adsorbed onto the crystals [7] and possibly desorbed due to the ultrasonic irradiation, resulting in a particular shape from the anisotropic process.

SEM images of $PbWO_4$ are shown in Fig. 2. These are especially well-defined, complex and highly ordered. They are structurally similar to those prepared by wet chemical methods without sonication [15] but the current structures are more highly ordered. At the pH of 6.54 and for 1 h ultrasonic irradiation (Fig. 2a), the product is composed of six tree trunk like structures at right angle. Two pairs are in the same plane. One pair is shorter than the other. The third pair is at a right angle to the four-trunk structure. One trunk is on the top and the other is at the bottom. Sometimes the trunks were released by ultrasonic irradiation. The structure is complex, uniform and systematic. The trunks are in the shape of pine trees and have arrowhead-shaped tips. When the ultrasonic irradiation was prolonged (Fig. 2b–d), the trunks became longer. Some structures were broken and some side grains were released (marked with a circle in Fig. 2d). For the preparation without the use of a surfactant, the product (Fig. 2e) is in the shape of seaweed and resembles those of Liu et al. [15]. This demonstrates that *N*-cetyl pyridinium chloride plays the role in the product morphologies and functions as the shape director of the process. In addition, $PbWO_4$ crystals prepared using a variety of the pH values with 1 h irradiation (Fig. 2f–j) have different morphologies. They have corn-like shape for the pH of 3 and 5, pine tree structure for the pH 7, granular shape for the pH 9, and irregular shape and size particles in clusters for the pH 11. At the pH above 11, lead hydroxide complex instead of $PbWO_4$ is probably formed due to the high OH^- concentration. These results show that the pH value plays the role in the shape

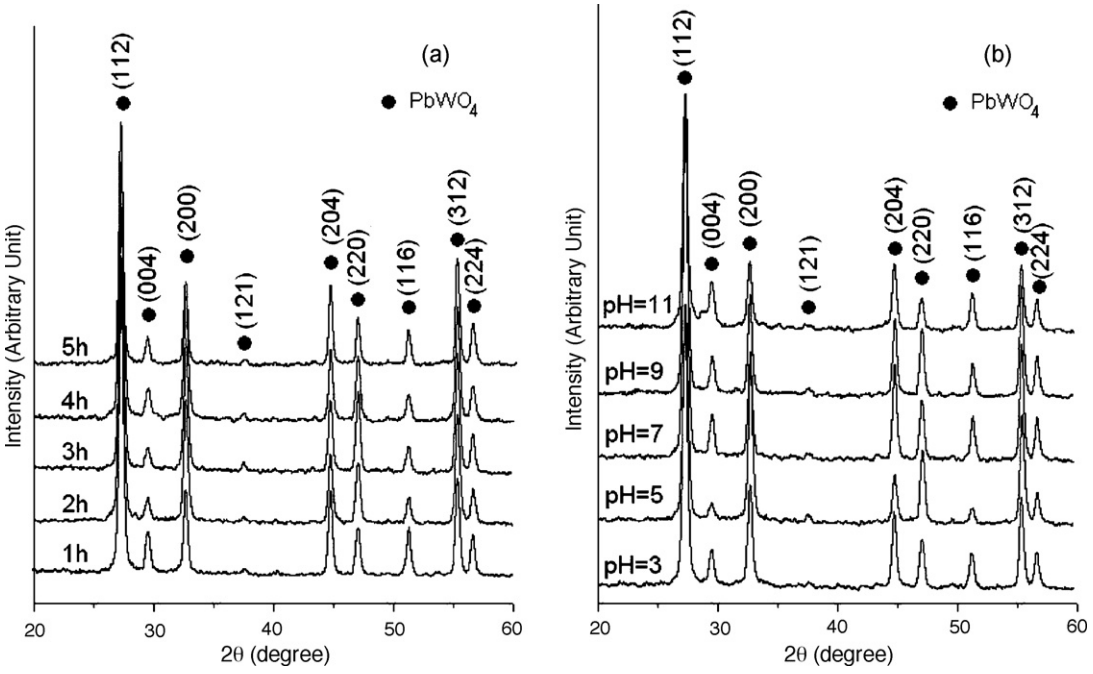

Fig. 1. XRD spectra of the products prepared in the solution containing *N*-cetyl pyridinium chloride using (a) the pH of 6.54 for different irradiation times and (b) the 1 h irradiation with different pH values.

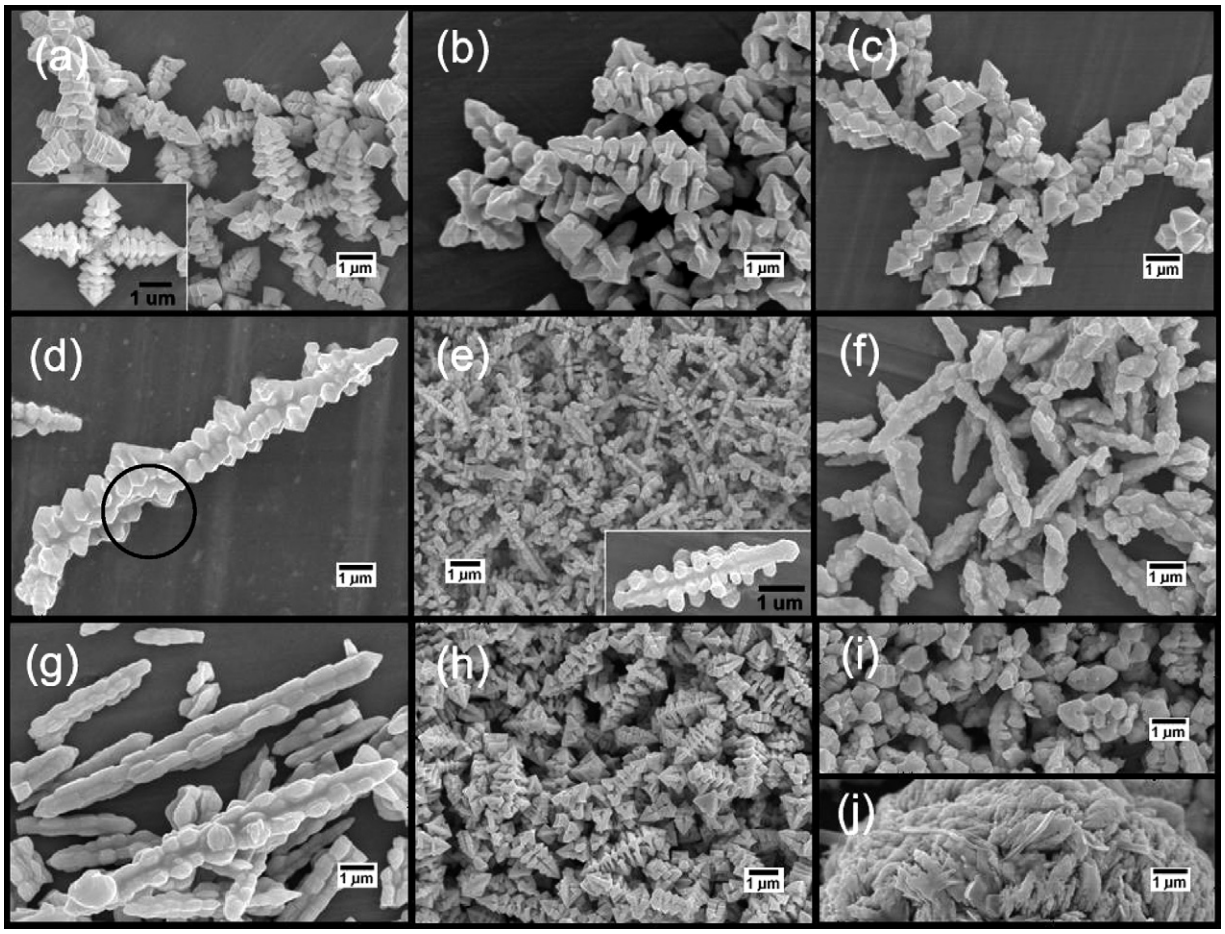

Fig. 2. SEM images of $PbWO_4$ prepared in (a–d) the solution containing *N*-cetyl pyridinium chloride (pH 6.54) with 1, 2, 3 and 5 h irradiations, (e) the surfactant-free solution (pH 6.26 and 1 h irradiation), and (f–j) the solution containing *N*-cetyl pyridinium chloride with the pH of 3, 5, 7, 9 and 11 (1 h irradiation), respectively.

and size of the products as well. At 1 h irradiation, the structures for the pH 6.54 (Fig. 2a) and 7 (Fig. 2h) are in the shape of a pine tree and are very similar.

Close examination of the TEM image of $PbWO_4$ prepared at pH 6.54 with 1 h of irradiation (Fig. 3a) shows the trunk of the product shaped like a pine tree which slopes up to a point. It has two halves that are the same in size and shape. SAED patterns (Fig. 3b and c) at two positions marked with a square and an ellipse on the product were interpreted [16–19]. The patterns correspond to $PbWO_4$ with tetragonal crystal system [14]. For the present research, zone axes [18–20] are in the [0 0 1] and $[0\,\bar{1}\,0]$ directions for the analyses at the square and ellipse, respectively. Each of them is parallel or nearly parallel to the electron beams. Diffraction patterns for $PbWO_4$ with [0 0 1] and $[0\,\bar{1}\,0]$ zone axes were simulated [13] and are shown in Fig. 3d and e. They are very symmetric and systematic. The a^*, b^* and c^* reciprocal lattice vectors for both patterns are in the [1 0 0], [0 1 0] and [0 0 1] directions, respectively. For one crystal structure, the corresponding lattice vectors are the same although their zone axes are different. Comparisons between the SAED and simulated patterns, they are in good accordance.

FTIR and Raman spectra of $PbWO_4$ with tetragonal stolzite structure are shown in Fig. 4. For the pH of 6.54 and different irradiation times (Fig. 4a), very strong W–O stretching bands of WO_4 tetrahedra were detected over the range 779–787 cm^{-1} [21–24]. O–H stretching and O–H bending bands of residual water were detected over the range 3302–3642 and 1654–1656 cm^{-1}, respectively. Comparisons to FTIR spectrum of *N*-cetyl pyridinium chloride (result not shown) reveal very weak bands of the surfactant at 2922 and 2852 cm^{-1}. At 1 h ultrasonic irradiation and different pH values (Fig. 4b), O–H stretching, O–H bending and W–O stretching bands were detected in the same way as the above. At the pH of 3, six vibrating bands of the surfactant were detected at 2922, 2852, 1631, 1486, 1175 and 478 cm^{-1}. The surfactant intensities decreased with the increase in the pH values. They were no longer detected at pH of 9 and 11. For pH 5, asymmetric and symmetric COO stretching bands of carboxylate group [25] were also detected at 1513 and 1410 cm^{-1}.

Raman spectra (Fig. 4c and d) revealed the presence of six vibrating bands over the range 100–1000 cm^{-1} although their morphologies are different. The $\nu_1(A_g)$, $\nu_3(B_g)$ and $\nu_3(E_g)$ specified as WO_4 stretching vibrations [2,22] were detected at 907.5, 768.5 and 752.7 cm^{-1}, respectively. The $\nu_1(A_g)$ has the strongest intensity. The $\nu_2(A_g)$ was detected as a strong band at 326.8 cm^{-1} with a weak band of $\nu_2(B_g)$ at 358.3 cm^{-1} [1,2]. They are the WO_4 bending vibrations [22,26]. The 176.9 cm^{-1} wavenumber is specified as a translational band of WO_4 groups

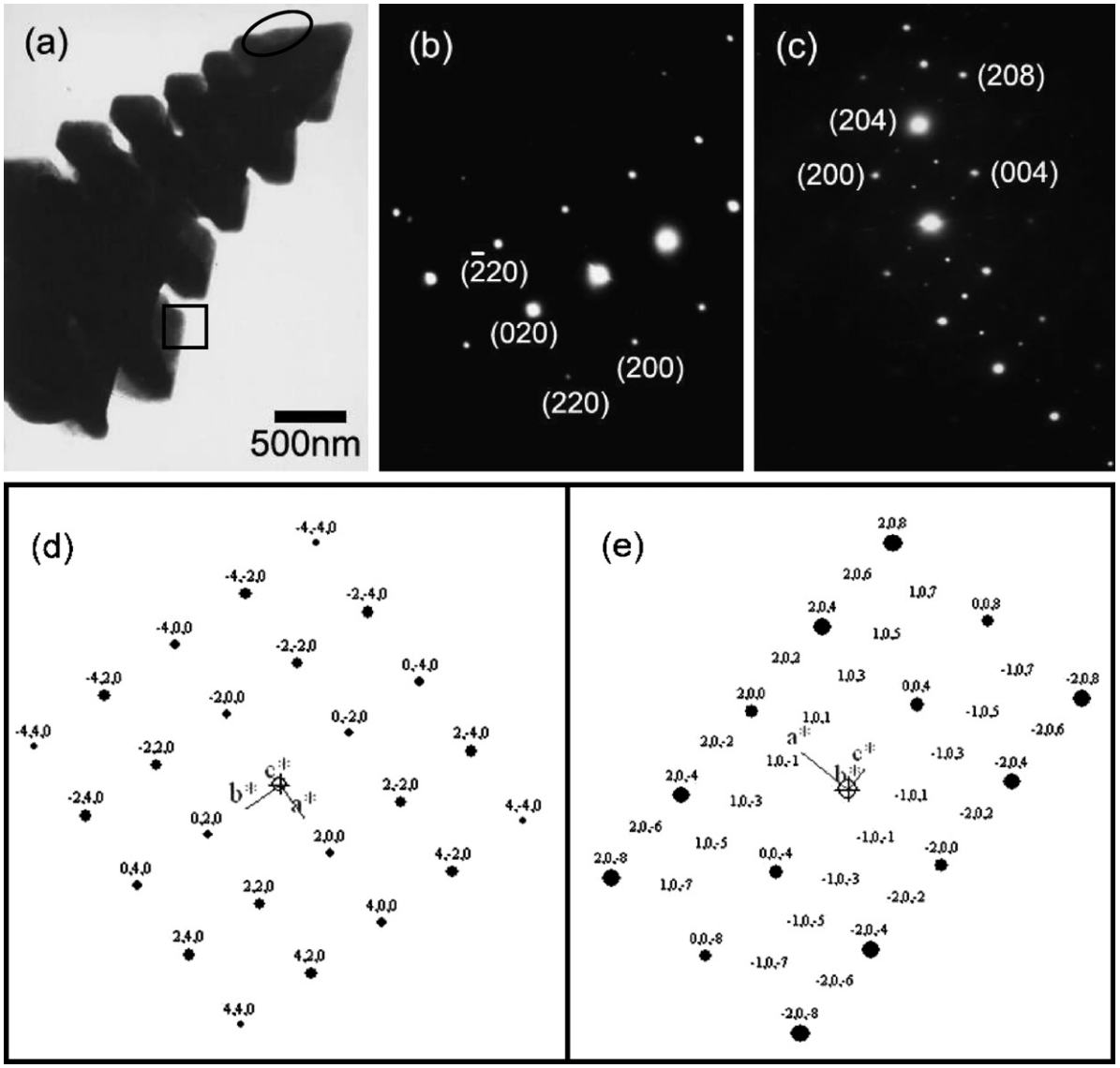

Fig. 3. (a) TEM image of $PbWO_4$ prepared in the solution containing *N*-cetyl pyridinium chloride (pH 6.54) with 1 h irradiation. (b–e) SAED and simulated patterns at the square and ellipse on the product, respectively.

[1,2]. There are some differences in the vibration frequencies, depending on the preparation processes and others.

The crystal-field splitting and hybridization of the molecular orbitals of $(WO_4)^{2-}$ tetrahedra [27] are shown in Fig. 5. The W 5d(t_2) and W 5d(e) orbitals are hybridized with the O 2p(σ) and O 2p(π) ligand orbitals to form $(WO_4)^{2-}$ tetrahedra. The four ligand p(σ) orbitals are compatible with the tetrahedral representation for a_1 and t_2 symmetries and the eight ligand p(π) orbitals are for t_1, t_2 and e symmetries. The top occupied state has t_1 symmetry formed from O 2p(π) states. The lowest unoccupied state has e symmetry formed from a combination of the W 5d(e) and O 2p(π) orbitals to give antibonding (*). The hybridization between the W 5d and O 2p orbitals is specified as covalent bonding between the ions. For ground state system, all one-electron states below band gap are filled to give a many-electron $^1A_1$ state. At the lowest excited state, there are one hole in t_1 (primarily O 2p(π)) state and one electron in e (primarily W 5d) state which give rise to many-electron $^1T_1$, $^3T_1$, $^1T_2$ and $^3T_2$ states. Among them, only $^1T_2 \rightarrow {}^1A_1$ transition is electric dipole allow [27,28].

For the present research, luminescence of the pine tree product is the strongest. Photoluminescent (PL) spectra of $PbWO_4$, the shape of a pine tree (Fig. 6), are very similar due to the similarity in the morphologies [5,8]. The PL emission is 415.5 nm wavelength due to the $^1T_2 \rightarrow {}^1A_1$ transition [27,28] of $(WO_4)^{2-}$ anions [8,9] in the blue range. The PL property is suitable for photoelectronic applications. Different morphologies can play the role in the difference of band gap and wavenumber. For instance, the emission wavenumbers of polyhedra, spindle-like and dot-shaped $PbWO_4$ nanostructures were detected at 493, 491 and 483 nm, respectively [2]. Dot-shaped $PbWO_4$ has the lowest wavenumber due to the smallest dimension. Crystallinity promotes PL intensity as well [2]. The polyhedral crystal is likely to contain the largest number of defects which lead to the highest PL intensity [2]. Comparing the macro- and nano-particles of $PbWO_4$, the first showed

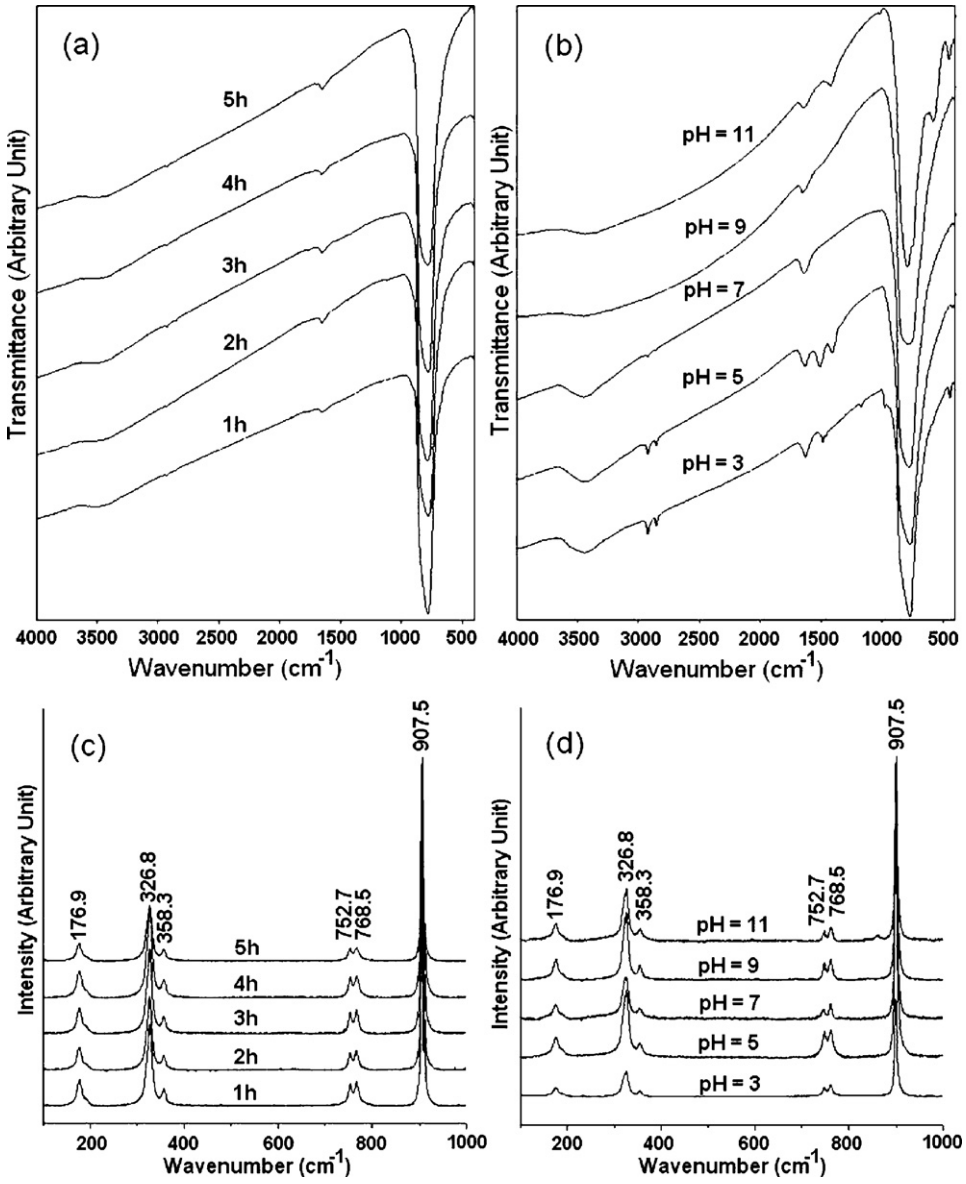

Fig. 4. (a and b) FTIR and (c and d) Raman spectra of $PbWO_4$ prepared in the solution containing *N*-cetyl pyridinium chloride using (a and c) the pH of 6.54 with 1–5 h irradiations, and (b and d) the 1 h irradiation with the pH of 3–11.

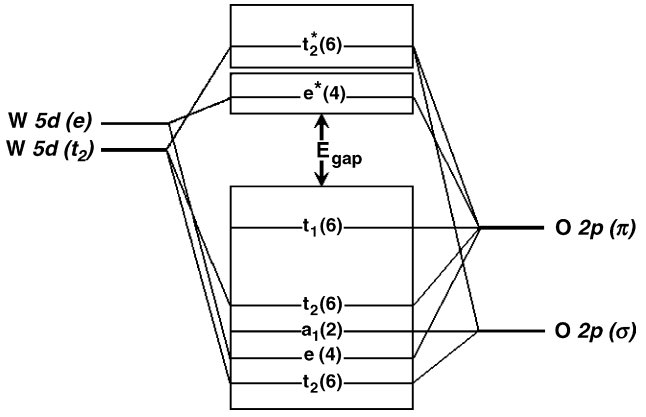

Fig. 5. Schematic diagram of the crystal-field splitting and hybridization of the molecular orbitals of $(WO_4)^{2-}$ tetrahedra. E_{gap} = energy band gap. *Antibonding (unoccupied) states. Degeneracy of each cluster state is specified as the figures in brackets [27].

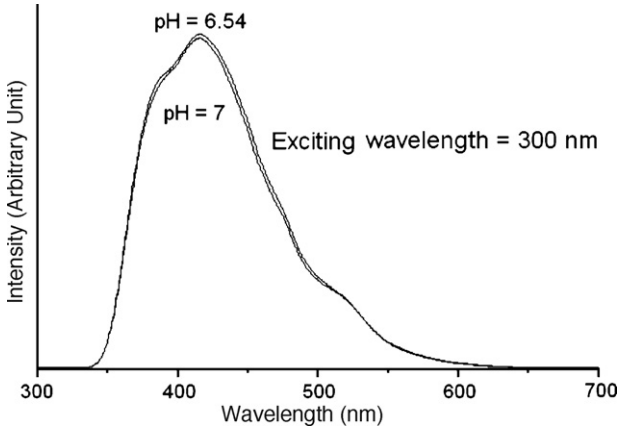

Fig. 6. PL spectra of $PbWO_4$ prepared in the solution containing *N*-cetyl pyridinium chloride using the pH of 6.54 and 7 with 1 h irradiation.

stronger blue emission than the second. The opposite is also true for the green emission [6]. The quantum sizes of particles influence their band gaps as well. For $CaWO_4$, band gap of bulk (2.95 eV, 421 nm) is smaller than that of nanofilm (3.03 eV, 409 nm) [21]. Photon energy emitted from the nanofilm is higher than that emitted from the bulk. It occurs a 12 nm blue-shift due to the quantum size effect [21].

4. Conclusions

$PbWO_4$ with different morphologies was successfully prepared from $Pb(OAc)_2{\cdot}3H_2O$, $Na_2WO_4{\cdot}2H_2O$ and *N*-cetyl pyridinium chloride by a sonochemical process. The final products, analyzed using XRD and SAED, were specified as pure $PbWO_4$ with tetragonal stolzite structure. SAED and simulated patterns are also in good agreement. The W–O stretching bands of WO_4 tetrahedra were detected by using FTIR at 779–787 cm^{-1} and Raman analysis at 907.5, 768.5 and 752.7 cm^{-1}. Their morphologies, characterized by SEM and TEM, were controlled by pH value, surfactant and irradiation times. They are corn-like, pine tree, granular and irregular in shape, depending on the reaction conditions. PL emission of the pine tree shaped products was detected at 415.5 nm due to the $^1T_2 \rightarrow {}^1A_1$ transition of $(WO_4)^{2-}$ tetrahedra.

Acknowledgements

We would like to give thank to the Thailand Research Fund (TRF), Commission on Higher Education (CHE), and Chiang Mai University (CMU) for financial support, and Dr. Richard Deming, Professor in Analytical Chemistry, Department of Chemistry and Biochemistry, California State University at Fullerton, California, U.S.A., for editorial assistance.

References

[1] J.Th. Kloprogge, M.L. Weier, L.V. Duong, R.L. Frost, Mater. Chem. Phys. 88 (2004) 438–443.
[2] J. Geng, J.J. Zhu, H.Y. Chen, Cryst. Growth Des. 6 (2006) 321–326.
[3] G. Zhou, M. L?, F. Gu, D. Xu, D. Yuan, J. Cryst. Growth 276 (2005) 577–582.
[4] L. Huo, Y. Chu, Mater. Lett. 60 (2006) 2675–2681.
[5] D. Chen, G. Shen, K. Tang, Zh. Liang, H. Zheng, J. Phys. Chem. B 108 (2004) 11280–11284.
[6] G. Zhou, M. L?, B. Su, F. Gu, Zh. Xiu, Sh. Wang, Opt. Mater. 28 (2006) 1385–1388.
[7] X.L. Hu, Y.J. Zhu, Langmuir 20 (2004) 1521–1523.
[8] J.H. Ryu, S.M. Koo, D.S. Chang, J.W. Yoon, Ch.S. Lim, Kw.B. Shim, Ceram. Int. 32 (2006) 647–652.
[9] J.H. Ryu, J.W. Yoon, Kw.B. Shim, Solid State Commun. 133 (2005) 657–661.
[10] Ch. An, K. Tang, G. Shen, Ch. Wang, Y. Qian, Mater. Lett. 57 (2002) 565–568.
[11] J. Geng, J.J. Zhu, D.J. Lu, H.Y. Chen, Inorg. Chem. 45 (2006) 8403–8407.
[12] J. Geng, D.J. Lu, J.J. Zhu, H.Y. Chen, J. Phys. Chem. B 110 (2006) 13777–13785.
[13] C. Boudias, D. Monceau, CaRIne Crystallography 3.1, 17 rue du Moulin du Roy, F-60300 Senlis, France, 1989–1998.
[14] JCPDS software, Powder Diffract. File, JCPDS Internat. Centre Diffract. Data, PA 19073-3273, U.S.A., reference code: 85-1857, 2001.
[15] B. Liu, S.H. Yu, L. Li, Q. Zhang, F. Zhang, K. Jiang, Angew. Chem. Int. Ed. 43 (2004) 4745–4750.
[16] K.W. Andrews, D.J. Dyson, S.R. Keown, Interpretation of Electron Diffraction Patterns, 2nd ed., Plenum Press, NY, 1971.
[17] B. Fultz, J. Howe, Transmission Electron Microscopy and Diffractometry of Materials, 2nd ed., Springer, 2002.
[18] T. Thongtem, A. Phuruangrat, S. Thongtem, Mater. Lett. 61 (2007) 3235–3238.
[19] T. Thongtem, A. Phuruangrat, S. Thongtem, Mater. Lett. 62 (2008) 454–457.
[20] B.D. Cullity, Elements of X-ray Diffraction, 2nd ed., Addison-Wesley Publ. Co., MA, 1978.
[21] G. Zhang, R. Jia, Q. Wu, Mater. Sci. Eng. B 128 (2006) 254–259.
[22] R.L. Frost, L. Duong, M. Weier, Spectrochim. Acta Part A 60 (2004) 1853–1859.
[23] J.A. Gadsden, Infrared Spectra of Minerals and Related Inorganic Compounds, Butterworths, England, 1975.
[24] G.M. Clark, W.P. Doyle, Spectrochim. Acta 22 (1966) 1441–1447.
[25] B. Smith, Infrared Spectral Interpretation, CRC Press, NY, 1999.
[26] Y. Huang, Hy.J. Seo, Q. Feng, Sh. Yuan, Mater. Sci. Eng. B 121 (2005) 103–107.
[27] Y. Zhang, N.A.W. Holzwarth, R.T. Williams, Phys. Rev. B 57 (1998) 12738–12750.
[28] M.J. Treadaway, R.C. Powell, J. Chem. Phys. 61 (1974) 4003–4011.